Available on CMS information server

CMS CR -2013/425

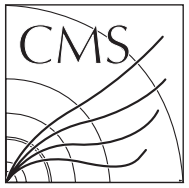

The Compact Muon Solenoid Experiment

Conference Report

Mailing address: CMS CERN, CH-1211 GENEVA 23, Switzerland

21 November 2013 (v2, 29 November 2013)

Sensor R&D for the CMS Tracker Upgrade for the HL-LHC

Hadi Behnamian for the CMS Collaboration

Abstract

At an instantaneous luminosity of $5 \times 10^{34} cm^{-2} s^{-1}$, the high-luminosity phase of the Large Hadron Collider (HL-LHC) is expected to deliver a total of 3000 fb^{-1} of collisions, hereby increasing the discovery potential of the LHC experiments significantly. However, the radiation environment of the tracking system will be severe, requiring new radiation hard sensors for the CMS tracker. The CMS tracker collaboration has almost completed a large material investigation and irradiation campaign to identify the silicon material and design that fulfills all requirements of a new tracking detector at HL-LHC. Focusing on the upgrade of the outer tracker region, pad diodes as well as fully functional strip sensors have been implemented on silicon wafers with different material properties and thicknesses. The samples were irradiated with a mixture of neutrons and protons corresponding to fluences as expected for various positions in the future tracker. The measurements performed on the structures include electrical sensor characterization, measurements of the collected charge and bulk defect characterization. In this paper, the performance and limitations of the different materials are presented.

Presented at *IPRD13 13th Topical Seminar on Innovative Particle and Radiation Detectors*

Preprint typeset in JINST style - HYPER VERSION

Sensor R&D for the CMS Tracker Upgrade for the HL-LHC

Hadi Behnamian[a] on behalf of the CMS Tracker Collaboration

[a] *School of Particles and Accelerators, IPM, Tehran, Iran*
E-mail: hadi.behnamian@cern.ch

ABSTRACT: At an instantaneous luminosity of $5 \times 10^{34} cm^{-2} s^{-1}$, the high-luminosity phase of the Large Hadron Collider (HL-LHC) is expected to deliver a total of 3000 fb^{-1} of collisions, hereby increasing the discovery potential of the LHC experiments significantly. However, the radiation environment of the tracking system will be severe, requiring new radiation hard sensors for the CMS tracker. The CMS tracker collaboration has almost completed a large material investigation and irradiation campaign to identify the silicon material and design that fulfills all requirements of a new tracking detector at HL-LHC. Focusing on the upgrade of the outer tracker region, pad diodes as well as fully functional strip sensors have been implemented on silicon wafers with different material properties and thicknesses. The samples were irradiated with a mixture of neutrons and protons corresponding to fluences as expected for various positions in the future tracker. The measurements performed on the structures include electrical sensor characterization, measurements of the collected charge and bulk defect characterization. In this paper, the performance and limitations of the different materials are presented.

KEYWORDS: HL-LHC; radiation hard sensors; tracking detector.

Contents

1. Introduction

The upgrade of the Large Hadron Collider (LHC), known as the High Luminosity-LHC [1], is scheduled for 2022. For this upgrade project, it is planned to achieve an integrated luminosity of up to 3000 fb^{-1} during its lifetime. This will cause a higher track occupancy and a much harsher radiation environment. From simulations of the radiation environment at CMS, one expects a maximum particle fluence of $1.5 \times 10^{15} n_{eq}/cm^2$ for the silicon strip tracker regions (shown in Fig. 1). Hence it is required to find radiation harder material and layouts and to increase the granularity of tracking detectors.

The CMS Collaboration started HPK [1] campaign to identify the future silicon sensor technology baseline for the phase II upgrade of the CMS tracker. To find irradiation hard materials, a large mixed protons and neutrons irradiation program has been set up for the materials of interest. These sensors have been irradiated to various fluences corresponding to different radii in the future tracker. The aim is to compare different materials and structures from one high quality producer. The main goals of the campaign are to identify the best material.

2. Measurement campaign overview

To investigate possible sensor technologies and materials, the CMS Tracker Collaboration has ordered a large number of 6 inch wafers from the producer HPK. These wafers were produced with different substrates, thicknesses, implants and geometries within this campaign. Also concerning the radiation hard material, three different silicon growth techniques with various oxygen contents have been used.

[1] Hamamatsu Photonics K.K.

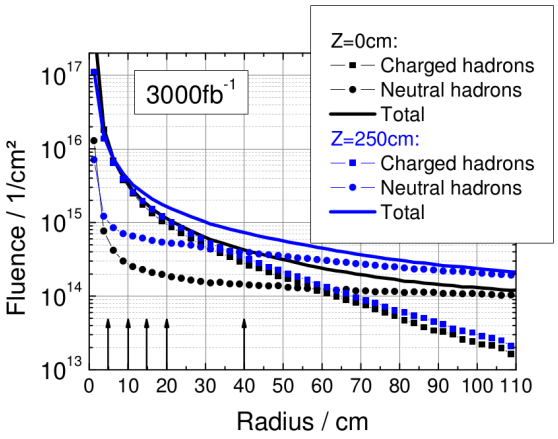

Figure 1. Simulated fluences by FLUKA for the CMS tracker dependent on the radius from the interaction point [2].

2.1 The wafer and materials

The common wafer layout has been designed with a variety of structures. Each wafer contains many test structures used for different purposes (Fig. 2), some important parts of which are introduced below [3].

- Diodes: Material properties and response to irradiation are investigated with different diodes. They are used to characterise the material through electric measurements (IV- and CV-curves) and also dark current for the detector is derived from the measurements on them.

- Test Structures: There are test structures to qualify and monitor the quality of the production process and determine operating parameters as well as mini sensors for beam tests and source measurements. The set of different test structures is called "halfmoon" within the community. Ten different measurements can be performed with this halfmoon structure. The interstrip parameters are taken from test structures consisting of strips. For the interstrip capacitance measurement, the bias ring is connected to the strips with a polysilicon resistor. This structure is labelled with CAP AC. In contrast, the interstrip resistance is determined with the CAP DC structure. As a polysilicon resistance would distort the interstrip resistance measurement, the strips of this structure are isolated from the bias ring. The coupling capacitance and dielectric break down voltage are determined with the CAP structure where the strips are also isolated from the bias ring.

- Baby sensors: Standard baby sensors are mounted which serve as reference mini-strip sensors. Mini-strip sensors evaluate radiation hardness of the different materials.

- Multi-Geometry strip sensors (MSSD): This article focuses on the MSSD which are highlighted with red rectangles in Fig. 2. The MSSD structure was used for beam tests and source measurements that contained 12 different regions with different strip pitches and width-to-pitch ratios. Strips are arranged in groups of 32 strips with different pitches from 70 to 240 μm. This kind of sensors could be used in the inner region of the Phase II strip tracker.

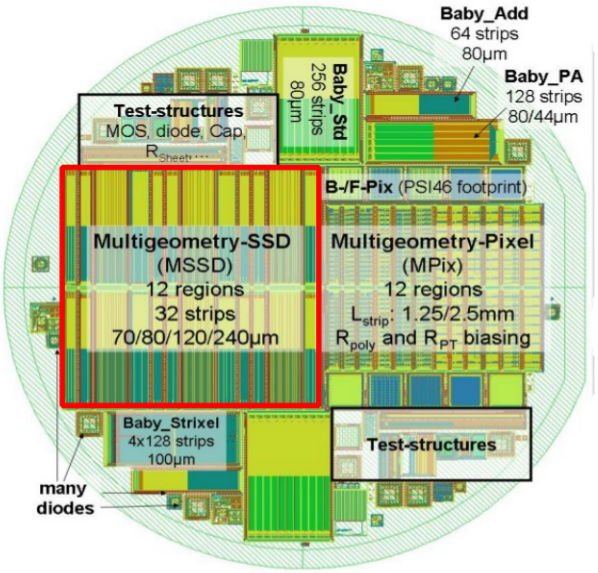

Figure 2. The HPK campaign wafer with the different structures.

These sensors allow for the actual assembly of modules and therefore investigation of the influence of geometry and materials on resolution, noise and signal-to-noise ratio. In this paper, charge collection and a new random ghost hits effect will be investigated.

- Multi-geometry pixel sensors: This structure is used for characterisation of a sensor with very short strips (1-2mm), varying pitch and biasing connection (poly-silicon or punch-through). The main focus of multi-geometry pixel structures are the capacitance measurements, as they lead to conclusions on the noise behaviour. One possible solution to cope with the higher track density would be the use of so called strixels, where the words strip and pixel are combined. These strixel sensors contain segmented strips with a larger area compared to the pixel detectors.

This layout with different active thicknesses has been processed by different technologies for the substrate production. It has been shown that silicon substrates with a high oxygen content show a higher degree of radiation tolerance. Therefore this campaign features materials with different oxygen concentrations:

- Float Zone (FZ): The best known material which serves as a reference and has also a high quality in terms of the high resistance values.

- Magnetic Czochralski (MCZ): This growth technique results in a high oxygen concentration in the silicon, which was shown to be beneficial in terms of radiation hardness.

- Epitaxial (Epi): This method allows to produce very thin (25-100 μm) active sensors by chemical vapour deposition of silicon on a carrier wafer.

For each type, p-strip implant in n-bulk material (n-type) and n-strip in p-bulk (p-type) were produced. For the n-in-p sensors, to avoid low interstrip resistances due to inversion layers, two different strip isolation technologies are tested. The sensor types named with letter P (p-stop) use a p+ layer between the n+ strips to intercept the electron accumulation layer, whereas sensor types labelled with the letter Y (p-spray) introduce a p doping on the full surface. In addition, wafers with a second metallization layer were also produced to investigate the radiation hardness and the noise behaviour with directly connected electronics.

To investigate the properties of sensors we have ordered various thicknesses. The float zone material is available in 320 and 200 μm physical thickness, 120 μm on carrier wafer and 320 μm thick with a reduction of active thickness (to 200 and 120 μm) by deep diffusion of the backside doping. The magnetic Czochralski material is physically 200 μm thick and the epitaxial wafers come in 50, 75 and 100 μm versions.

An advantage of thinner sensors is the lower depletion voltage compared to thicker sensors. After irradiation also trapping of charge carriers is reduced due to the reduced thickness and a higher electrical field. A reduction of the active thickness can be achieved with deep diffusion. The deep diffusion process allows to produce thin sensors at lower costs compared to the thinning process or wafer bonding. The active thickness is reduced but the physical thickness is still 320 μm, which allows easier handling than with thinner wafers, but a potential benefit for the material budget with thinner sensors would be abandoned. Labels for the materials for this paper are composed of silicon type (FZ: float zone with physical thickness of 320 μm and deep diffusion; MCZ: magnetic Czochralski; FTH: thinned float zone), nominal active thickness (320, 200 μm) and doping type (N: n-bulk; P: p-bulk with p-stop; Y: p-bulk with p-spray).

2.2 Irradiation

The expected fluence, which will be reached after the high luminosity upgrade of the LHC, has been calculated. The radial dependence of neutral and charged hadron fluences differs significantly (Fig. 1), which leads to a variation of the ratio of charged to neutral hadrons as a function of radius. It was found that neutrons, protons and mixed irradiations lead to different effects in different materials. Therefore we need to probe these effects on our materials in a consistent way. Since we cannot survey the conditions in the entire tracker volume, we picked some representative points as summarized in Table. 1.

Several irradiation steps have already been carried out and different materials were irradiated with 1 MeV neutrons from the reactor in Ljubljana and with 25 MeV protons from the cyclotron in Karlsruhe. Short term annealing is performed after every irradiation step. Additional annealing effects introduced during the transport from the irradiation facilities to the individual institutes, where the measurements are performed, have to be considered.

3. Measurement setup and results

Some strip properties like signal (charge collection) and noise were determined in laboratory measurements by using the actual CMS readout system. For testing purposes, the sensors were

Radius	Protons / 10^{14} $n_{eq}cm^2$	Neutrons / 10^{14} $n_{eq}cm^2$	Total / 10^{14} $n_{eq}cm^2$	Ratio p/n
40 cm	3	4	7	0.75
20 cm	10	5	15	2.0
15 cm	15	6	21	2.5
10 cm	30	7	37	4.3
5 cm	130	10	140	13

Table 1. Summary of the foreseen particle fluences for this campaign. This table shows the planned fluence points for the irradiations at the given radii of the future CMS tracker.

mounted on an aluminium plate and wire bonded to APV25 readout chips [4]. To study signal and noise measurements, these MSSD modules are exposed to particles from a radioactive beta source (^{90}Sr). In the next two parts, we will examine these measurements by varying bias voltage, fluence, annealing time and temperature for different geometries.

3.1 Charge collection

The signal to noise ratio is the most important parameter for hit identification. The collected charge was measured throughout the collaboration using radioactive beta source. These distributions were fitted with the convoluted Landau and Gaussian function which reproduced the histograms very accurately. From the fit, the most probable value (MPV) was extracted. In this section, we want to discus about this parameter at some fixed applied bias voltage as a function of fluence and annealing time for different materials.

Fig. 3 shows the degradation of the collected charge for FZ320μm materials at 600V and 900V reverse bias (n-bulk on the left and p-bulk on the right). These measurements have been done for different irradiations up to $1.5 \times 10^{15} n_{eq}/cm^{-2}$, which is the highest expected fluence. The initially higher signal of the thick materials drops fast with increasing fluence. To make a comparison between CMS and ATLAS results, we put ATLAS results ([5] and [6]) into the same plot with equivalent doses of neutron and proton irradiations. In general, it has been found that for n-bulk materials (left side of Fig. 3), CMS measured higher signal than ATLAS but it must be noticed that these two experiments used sensors with different actual thicknesses. Also there are some differences between vendors and irradiation types (ATLAS results with only neutron irradiations while CMS used mixed ones). The CBC (CMS binary chip) threshold is expected to be between 4000 and 6000 electrons, thus we consider a 8000 electrons to be acceptable as signal. From that plot, it is apparent that N-bulk strip sensors could be used for fluences below $7 \times 10^{14} n_{eq}/cm^{-2}$, but after that one can observe a strong decrease in cluster charge below the CBC threshold. Then this kind of sensors would not be useful for higher irradiation scenarios at phase II tracker upgrade.

In the case of FZ320μm p-bulk material (right side of Fig. 3), the behaviour of collected charge after irradiation is consistent for all thick sensors. The cluster charge for this case shows a uniform drop trend. Our measurements on these strip sensors show a signal higher than 8000 electrons even after high irradiation fluences of $1 \times 10^{15} n_{eq}/cm^{-2}$. This level of signal-to-noise is sufficient for

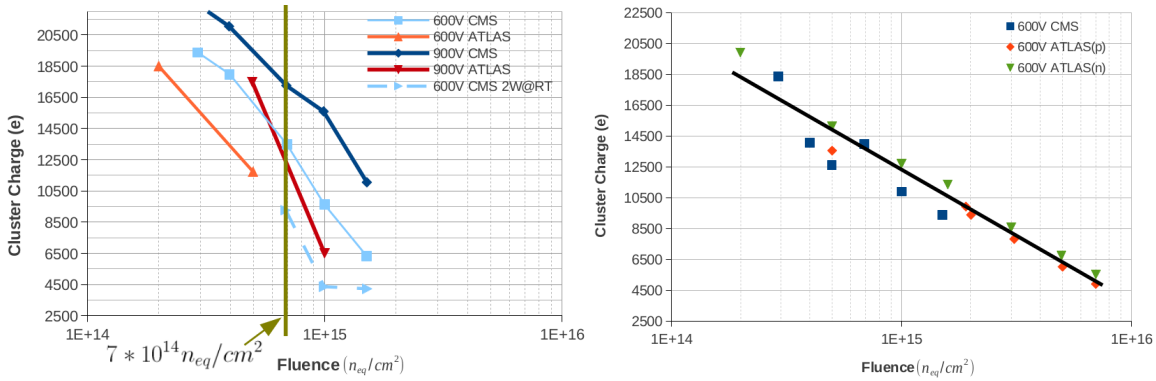

Figure 3. CMS and ATLAS collected charge vs. irradiation fluence for FZ320um (n-bulk on the left and p-bulk on the right). CMS measurements have been taken at $-20°C$ with a ^{90}Sr beta source by using APV25 read-out system. A cluster has been defined so that a seed and neighbors signals are bigger than three and two times the strip noise, respectively.

high signal efficiency and low noise occupancy. The left part of Fig. 4 shows the seed charge for all thin materials with 200 μm thickness at fixed bias voltage of 600V without any annealing. From that plot, it seems for fluence below $7 \times 10^{14} n_{eq}/cm^{-2}$, n-bulk sensors have higher seed signals with respect to p-bulk ones. Then n-bulk strip sensors could still be used in this range of fluence. As can be deduced from the plot, in the case of higher irradiation levels, the collected charge for n-bulk materials were not high enough to be taken into account as signal. The comparison results for FZ material between different thicknesses (200 and 320 μm) are shown on the right side of Fig. 4. It can be seen that after higher fluence of $1 \times 10^{15} n_{eq}/cm^{-2}$, the physically thin materials collect comparable or even slightly more charge than the thick sensors. Thus 200 μm thick strip sensors allow to reduce the material budget and keep the charge collection at the same level as 320 μm thick sensors at high fluence.

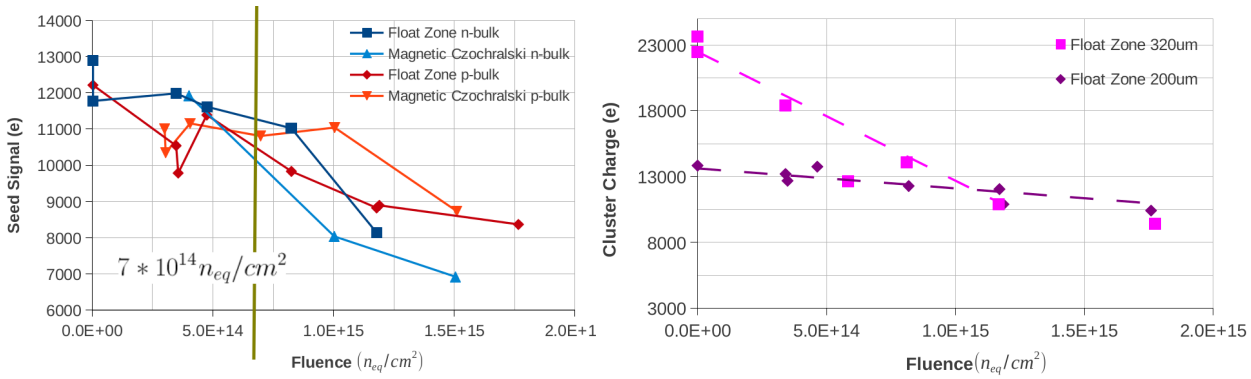

Figure 4. Left: charge collection vs. irradiation fluence for FZ200μm p and n-bulk materials. Right: charge collection comparison between thick (320 μm) and thin (200 μm) FZ sensors. Both of them are measured at fixed bias voltage of 600V without any annealing.

Fig. 5 shows the dependence of the seed signal on annealing time, for fixed fluences and different materials and thicknesses.. These two plots are related to medium fluence ($7 \times 10^{14} n_{eq}/cm^{-2}$) and

high irradiation level ($1 \times 10^{15} n_{eq}/cm^{-2}$) for devices that were temperature annealed. For both of them, signal is more stable for p-bulk sensors than n-bulk ones. In the case of medium level, all thin p and n-bulk samples work well and show seed signals bigger than 8000 electrons even with high amount of annealing (20 weeks at room temperature). But for high irradiation (right side of Fig. 5), signal on n-bulk sensor decreases after a few weeks at room temperature to a low level. This is one reason why p-bulk will be the best choice for the outer part of the tracker at the phase II upgrade project. This effect is also most pronounced for Magnetic Czochralski material, which also has a higher signal with annealing than Float Zone especially at higher fluences.

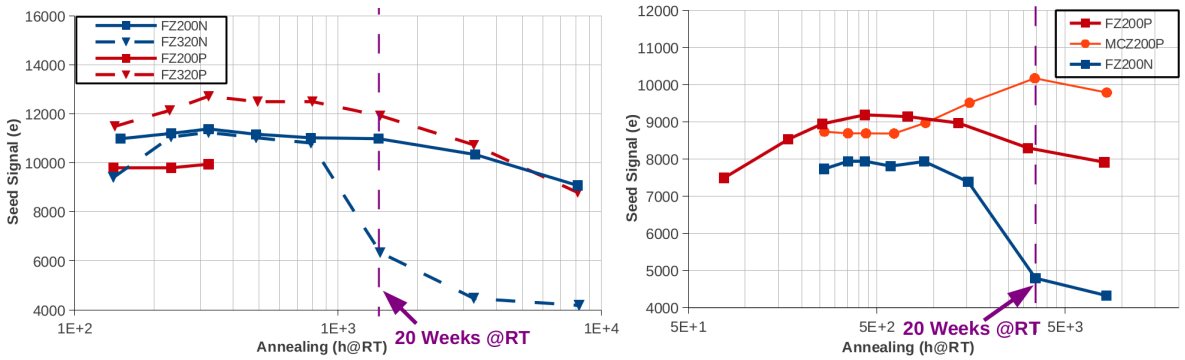

Figure 5. Annealing behaviour of seed signal at fixed bias voltage equals to 600V for two different irradiation levels. Left: medium fluence ($7 \times 10^{14} n_{eq}/cm^{-2}$) and Right: high fluence: ($1 \times 10^{15} n_{eq}/cm^{-2}$).

3.2 Study of random ghost hits

The higher fluences could damage the sensors and increase their leakage current, the depletion voltage and charge carrier trapping. The higher leakage current causes higher noise and more heat load. Hence it is required to study noise distributions of different materials at higher fluences. It is expected that the noise follows a Gaussian distribution before and after irradiation, but CMS has observed that the noise distributions have large non-Gaussian tails (see Fig. 6). These fake hits have been created especially for irradiated n-bulk sensors at higher bias voltages and lead to strip occupancies of more than 1% even if no particles are crossing the sensor. To take into account these new effects, we defined two methods, as illustrated in Fig. 6. We extracted 5σ cuts by fitting noise distributions with Gaussian functions. In the first method, the strip occupancy is defined as the number of signals exceeding 5σ cuts at positive side band divided by the number of strips and the number of events (middle plot at Fig. 6). In the second definition, we built fake hits as subtraction of signals exceeding 5σ cuts at two side bands divided by the number of strips and the number of events (right plot at Fig. 6). The strip occupancy due to non-Gaussian noise hits depends on bias voltage, fluence and annealing time. To study this effect we made a phase space scan of those parameters and extracted the fake hits rate.

Fig. 7 shows the strip occupancy due to noise hits (by using the first method) as a two dimensional function of bias voltage and annealing time. It can be seen that no effect appeared in p-bulk sensors even after mixed irradiation (top-left part), while these measurements show visible effects for n-bulk materials for every irradiation type. Also after longer annealing of about 90 days, the rate

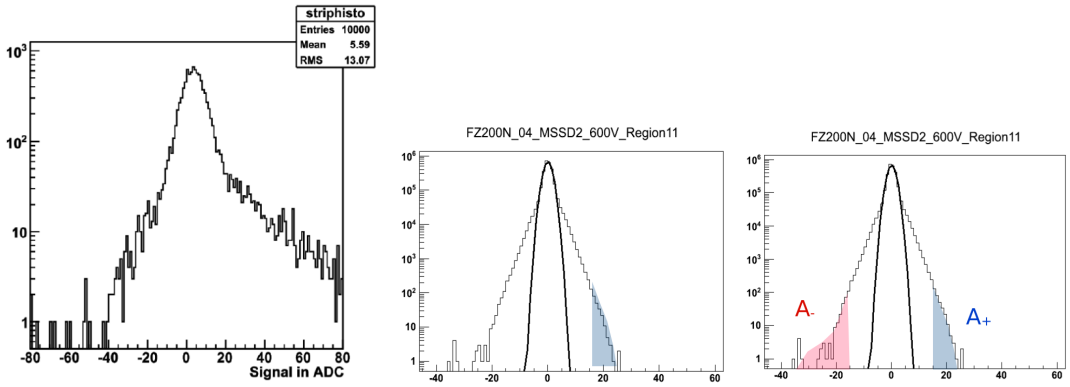

Figure 6. Left: Example of pedestal-subtracted noise distribution in irradiated n-type strip sensors taken from Ref. [3]. Middle and Right: Two different definitions of the fake hits rate.

of strip occupancy is going down again. In case of only neutron irradiated n-bulk sensors (top-right side), higher bias voltages of about 800V are needed to produce fake hits. This effect is less pronounced for neutron irradiation compared to irradiation with charged hadrons (see bottom side of Fig. 7). For higher mixed irradiation levels, this effect starts even at low voltages of about 300 V. This difference of charged and neutral hadron irradiations indicates that ionising energy loss in the SiO_2 interface might be relevant. This dependence on ionizing radiation hints towards a combined effect of bulk damage and surface charge. Simulation on surface and bulk damages can help to study this effect in more detail.

Before studying the simulation of this effect, we have investigated fake hit contributions for different geometries (different strip width and pitches). To study random ghost hits on different geometries we used MSSD with 12 regions depicted on the left side of Fig. 8. We measured the voltage for which the random ghost hits appeared (called turn-on voltage) for all of the materials in different regions. It can be noticed that the second definition of fake hits rate was assumed for this study. Fig. 8 shows the turn-on voltage for a variety of materials at different irradiation levels with different strip width and pitches. It can be seen that this effect has not appeared for p-bulk sensors with 200 μm thicknesses even at higher bias voltage. The other consequence is that regions with high strip pitches are affected earlier.

3.3 Device simulation

To investigate this new random ghost hits effect, it seems necessary to study device simulation. It can be shown that we have some correlations between fake hits results with simulation of electric field intensity below the SiO_2 layer. First simulations which take into account both the bulk defects generated by non-ionising energy loss and the increased oxide charge density due to ionising energy loss show very high electric fields close to the p+ strip implants for n-type sensors. An oxide charge density of $1.2 \times 10^{12} cm^{-2}$ is assumed and bulk defects are implemented which correspond to a fluence of $1 \times 10^{15} n_{eq}/cm^{-2}$. The electric field intensity at 0.1 μm below the SiO_2 layer is shown on the left side of Fig. 9. This is the first correlation between simulation and measurements, because as mentioned earlier only for n-bulk materials the fake hits effect was observed. Simulations show higher electric fields at the strip edges for irradiated n-bulk while no field peaks are seen for p-bulk

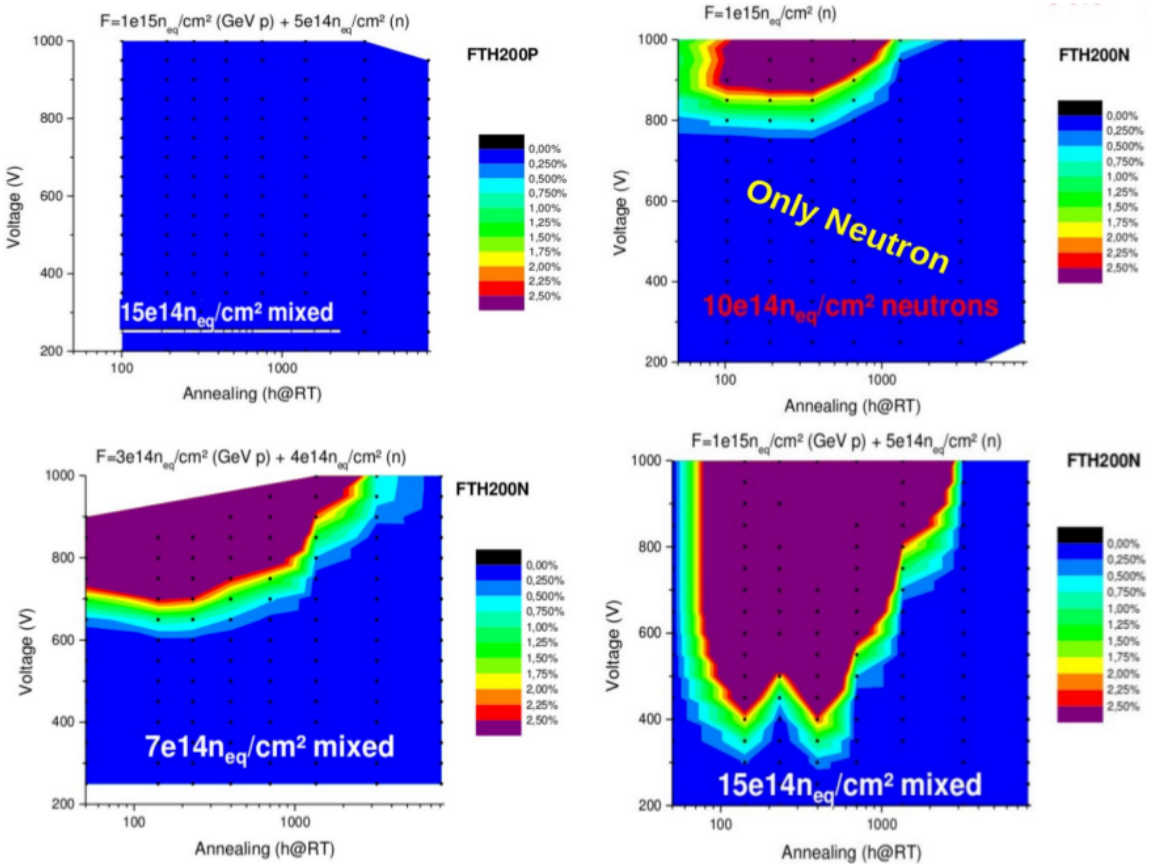

Figure 7. Strip occupancy due to random noise hits as a function of bias voltage and annealing time after irradiation. Top-left: p-bulk, Top-right: n-bulk with only neutron irradiation, Bottom: n-bulk with two different mixed irradiation levels.

materials. Also lowering the values used for oxide charge concentration decreases the peak value of the electric field in n-type sensors (middle plot of Fig. 9). And this would explain why random ghost hits are reduced for only neutron irradiation with less ionization (second correlation). As shown in Fig. 8, regions with high strip pitches are affected earlier. This could be confirmed with simulation as shown on the right side of Fig. 9. From simulation, it is apparent that these regions have higher electric field peaks than others (third correlation).

4. Summary and outlook

To find the best choice material for CMS outer tracker at high luminosity LHC, signal and noise were studied on sensors produced within the HPK campaign. To reach this goal, sensors were irradiated to fluences expected at radii of 20 and 60 cm. The output of the measurements can be summarized as follows:

- n vs. p-bulk materials: For medium irradiation, n-bulk materials give higher signals, but at higher fluences the p-bulk sensors collect more charge carriers. Signal on n-bulk materials is decreased after a couple of weeks at room temperature while charge collection is rather

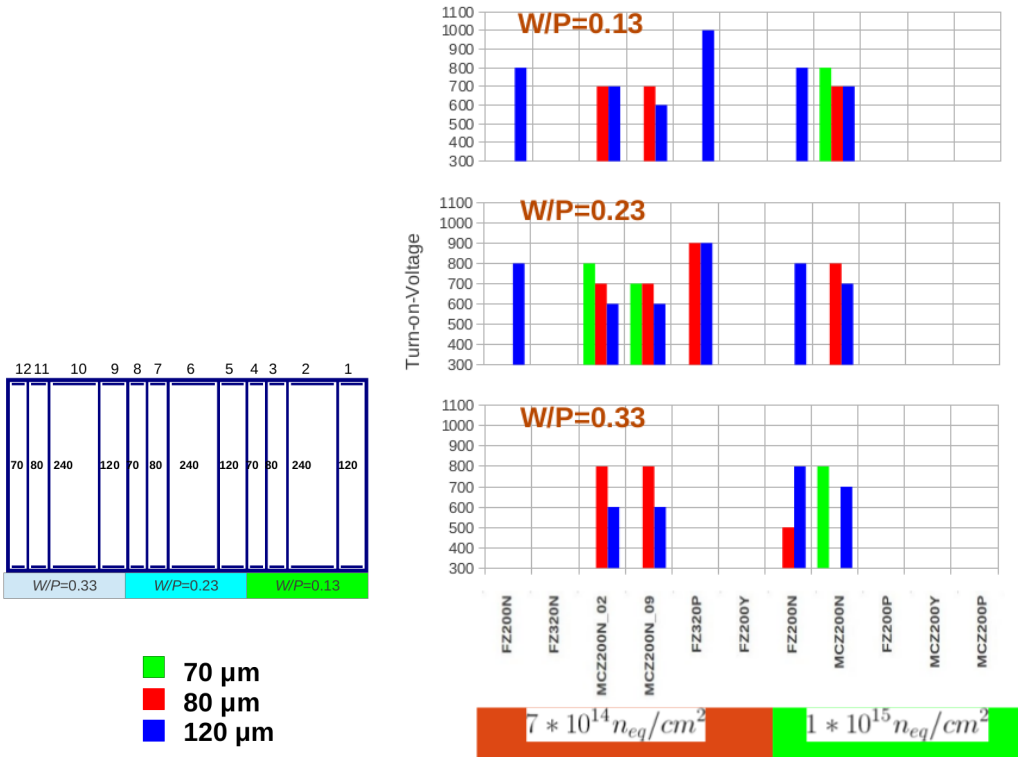

Figure 8. Left: Feature of MSSD with 12 regions. Every region has another combination of strip width and pitch, and is shown with different color labels. Right: Turn-on-voltage for present materials with different fluence, strip width and width-to-pitch ratios.

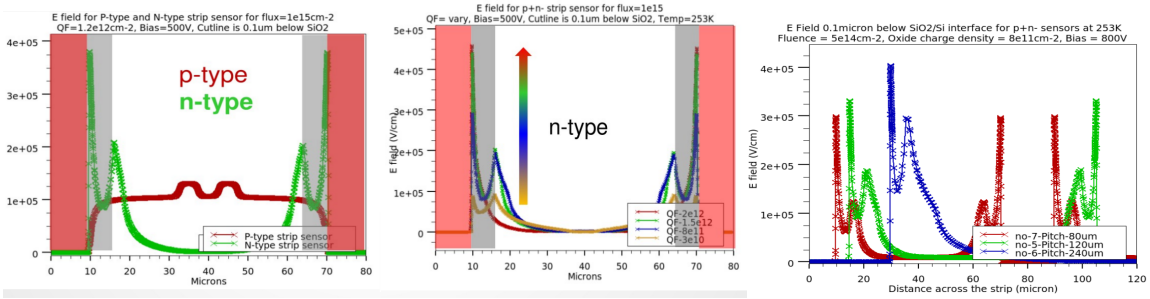

Figure 9. Electric field intensity simulation at 0.1 μm below the SiO_2 layer (see Ref. [7]).

stable for p-bulk sensors. Also as we mentioned for n-bulk, fake hits are created and increase the strip occupancy. This new effect could be explained with device simulation of the electric field and needs to be studied further.

- Float zone vs. Magnetic Czochralski: Sensors made of MCZ silicon show an increased signal with annealing. Operation of MCZ sensors would enable annealing scenarios with longer annealing times and hence with lower dark current, less power consumption and lower heat generation.

- 200 vs. 320 μm thickness: The collected charge was comparable for both of them especially

for sensors that will be located at a radius of 20 cm. Thinner strip sensors allow to reduce the material budget and keep the charge collection at the same level as 320 μm thick sensors especially at high fluences.

Finally due to the good charge collection performance of the p-bulk materials after the expected fluences, and since no non-Gaussian noise hits were observed for them, CMS decided to use p-bulk sensors for the tracker and concentrate the future work on optimizing the technology and the geometry.

Acknowledgments

The research leading to these results has received funding from the European Commission under the FP7 Research Infrastructures project AIDA, grant agreement no. 262025.

References

[1] F. Gianotti et al., *Physics potential and experimental challenges of the LHC luminosity upgrade*, Eur. Phys. J C39 (2005) 293.

[2] S. Muller, *The Beam Condition Monitor and the Radiation Environment of the CMS Detector at the LHC*, Karlsruhe Institute of Technology, IEKP-KA/2011-1, CMS TS-2010/042 (2011).

[3] A. Dierlamm, *Characterisation of silicon sensor materials and designs for the CMS Tracker Upgrade*, presented at 21st International Workshop on Vertex Detectors in Jeju, Korea (2012).

[4] M. Raymond et al., *LEB 2000*, CERN-2000-010 (2000).

[5] G. Casse et al., *Measurements of charge collection efficiency with microstrip detectors made on various substrates after irradiations with neutrons and protons with different energies*, PoS(VERTEX 2008) 036.

[6] G. Casse et al., *Evidence of enhanced signal response at high bias voltages in planar silicon detectors irradiated up to* $2.2 \times 10^{16} n_{eq}/cm^{-2}$, Nuclear Instruments and Methods A 636 (2011), S56-S61.

[7] R. Ranjeet et al., *Simulations for Hadron Irradiated n+p- Si Strip Sensors Incorporating Bulk and Surface Damage*, presented at 23rd RD50 Workshop, CERN (2013).